

Ultralong-range Casimir-Lifshitz forces mediated by nanowire materials

Stanislav I. Maslovski* and Mário G. Silveirinha

*Departamento de Engenharia Electrotécnica Instituto de Telecomunicações,
Universidade de Coimbra Pólo II, 3030-290 Coimbra, Portugal*

(Received 29 December 2009; published 25 August 2010)

Here, we show that the Casimir-Lifshitz force (either attractive or repulsive) between two planar material slabs embedded in a dense array of silver nanowires is an ultralong-range force that decays with the separation of the bodies, a , as $1/a^2$, whereas in an isotropic background it decays as $1/a^4$. It is demonstrated that the nanowires effectively channel the quantum fluctuations of the electromagnetic field through the region between the bodies, boosting in this manner the intensity of the Casimir force at long distances. Moreover, in a configuration involving a stationary planar slab and a spherical object able to slide within the nanowire background (e.g., an air bubble) the dependence of the force on the separation is shown to be $1/a$ as compared to $1/a^3$ in an isotropic background. Our theoretical calculations suggest that a significant repulsive Casimir force can be measured for distances up to 10 μm in such a scenario.

DOI: [10.1103/PhysRevA.82.022511](https://doi.org/10.1103/PhysRevA.82.022511)

PACS number(s): 31.30.jh, 42.50.Ct, 12.20.-m, 42.50.Lc

I. INTRODUCTION

The Casimir-Lifshitz [1–3] forces have a quantum origin and can be observed as attraction [4] or repulsion [5] between uncharged slabs of different materials. In a seminal work [1], Casimir studied the force acting on a pair of two perfectly conducting plates in a vacuum, and found that the force is attractive and decays as $1/a^4$ as the separation between the plates a is increased. Later, Lifshitz [2,3] generalized Casimir's results to slabs of arbitrary dielectrics, and it was soon realized that the force may be repulsive when the two slabs [with dielectric functions $\varepsilon_1(i\xi)$ and $\varepsilon_3(i\xi)$] are immersed in a fluid with dielectric function $\varepsilon_2(i\xi)$, such that $\varepsilon_1(i\xi) < \varepsilon_2(i\xi) < \varepsilon_3(i\xi)$. This theoretical finding has been supported by a recent experiment [5]. Recently, it was suggested that the Casimir interaction between structured materials may be repulsive [6–8]. However, in all these works Casimir's forces appear as extremely weak and relatively short-range forces, which are very hard to observe and to measure.

From Lifshitz's formula, the Casimir force can be calculated from the plane wave response of the material slabs to complex frequencies $\omega/c = i\xi$, being c the speed of light in vacuum [9,10]. The intensity of the force is mainly determined by the response of the slabs to plane waves associated with relatively small transverse wave vectors $\mathbf{k}_\parallel = (k_x, k_y, 0)$ because the attenuation constant in a vacuum is of the form $\gamma_0 = \sqrt{\xi^2 + k_x^2 + k_y^2}$, and thus increases quickly with k_\parallel . Curiously, such behavior (for $\omega/c = i\xi$) is completely analogous to that characteristic of evanescent plane waves associated with ω real valued. Even though for any isotropic dielectric material the propagation characteristics (particularly the attenuation constant) of modes with large transverse wave vector are strongly dependent on k_\parallel (for both real valued and imaginary frequencies), recently it was shown that the existence of evanescent waves is not an inevitability, and that it is possible to engineer the microstructure of a material in such a way that all the plane wave modes are propagating waves (for ω real valued). Specifically, several recent works demonstrated

that an array of nanowires enables the transport of complex electromagnetic images at long distances with subwavelength resolution [11,12]. The key property of such nanowire materials (uniaxial wire medium) is that the propagation constant of the fundamental electromagnetic mode is independent of the transverse wave vector \mathbf{k}_\parallel , and in particular, for ω real valued, the fundamental mode is always a propagating wave. It is thus natural to ask what will happen if the Casimir interaction between two material slabs is mediated by such wire medium. Indeed, since in wire media the propagation constant is nearly insensitive to k_\parallel , can the contribution of the modes with large k_\parallel to the Casimir force be greatly enhanced? In this work, we prove that the answer is affirmative, and that the intensity of the Casimir force may be dramatically increased at long distances, being the traditional $1/a^4$ behavior replaced by $1/a^2$, similar to structures that are inherently one-dimensional (1D) [9,13,14].

II. CASIMIR FORCE IN PARALLEL PLATE CONFIGURATIONS

Let us first consider the case of two conducting plates separated by a slab of uniaxial wire medium with thickness a (see the inset of Fig. 1). The wire medium is formed by parallel conducting rods (nanowires) oriented along the direction orthogonal to the plates (z axis), and arranged in a square lattice with period b [15]. We assume that $r_0 \ll b < a$, being r_0 the wire radius. To begin with, we will treat the wire medium as a continuous medium, using the homogenization model described in Refs. [15,16]. The homogenization model is applicable when $kb \ll 1$, being $k = \omega/c$. Ahead, in Sec. III, we will show that the continuous medium approach yields a value for the force that is very close to the exact value obtained by a full wave calculation that takes into account the granularity of the structure.

In general, there are three classes of eigenwaves in the uniaxial wire medium: waves with $E_z = 0$, $H_z \neq 0$ which are ordinary waves, or the transverse electric (TE) waves, waves with $E_z \neq 0$, $H_z = 0$ which are the usual extraordinary waves or the transverse magnetic (TM) waves, and waves with $E_z = 0$, $H_z = 0$ which are transverse electromagnetic (TEM) waves. Strictly speaking, the latter are quasi-TEM

*stas@co.it.pt

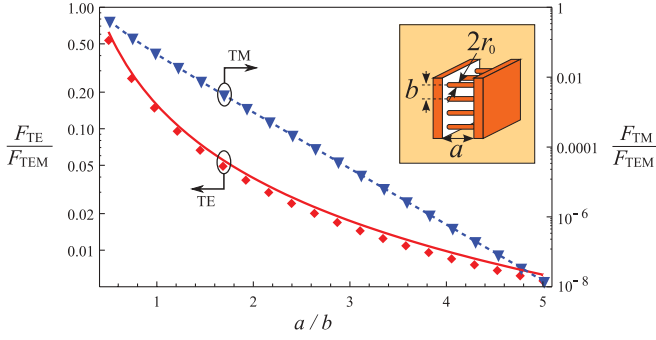


FIG. 1. (Color online) Normalized Casimir forces due to the TE (red solid line, left scale) and TM (blue dashed line, right scale) waves acting on a pair of conducting plates embedded in uniaxial wire medium as functions of the relative thickness of the slab (logarithmic scale). The radius of the wires is $r_0 = b/20$. The discrete symbols were calculated with full wave simulations (Appendix A).

waves, because in the presence of loss the longitudinal component of the electric field does not vanish completely. For simplicity, first we will assume that the wires are perfect electric conductors (PEC) (the effect of loss and dispersion in realistic metals will be considered in Sec. IV). Within the continuous medium approximation, the previously mentioned waves obey the following dispersion relations [15],

$$k_x^2 + k_y^2 + k_z^2 = k^2, \quad (\text{TE modes}), \quad (1)$$

$$k_p^2 + k_x^2 + k_y^2 + k_z^2 = k^2, \quad (\text{TM modes}), \quad (2)$$

$$k_z^2 = k^2, \quad (\text{TEM modes}), \quad (3)$$

where k_p is the plasma wave number, which may be estimated as $k_p = \sqrt{2\pi/\log[b^2/4r_0(b-r_0)]}/b$ [16]. Notice that the dispersion of the TEM mode is independent of k_x and k_y . This suggests that TEM eigenmodes associated with different k_x and k_y will contribute equally to the Casimir force, boosting its intensity. In the exact full wave model (not limited by the bounds imposed by homogenization theory), the metamaterial is modeled as a photonic crystal, and there is an infinite number of TE and TM modes, whose dispersion is of the form $k_z^2 = k^2 - \beta_i^2(k_x, k_y)$, where $\beta_i(k_x, k_y)$ is the cutoff wave number of the mode characterized by the index i and by the transverse wave numbers k_x and k_y .

In order to find the force acting on the plates, we consider a cavity that encloses the space between the plates with reflecting walls at $x = \pm L/2$ and $y = \pm L/2$. Therefore, the allowed wave numbers of the standing waves in the cavity are $k_x = \pi n_x/L$, $k_y = \pi n_y/L$, $k_z = \pi n_z/a$, where $n_{x,y,z}$ are non-negative integers. As is enforced by the boundary conditions, n_z starts at zero for the TM modes, and at unity for the TE and TEM modes. It is assumed that the wires are in electric contact with the plates (this is discussed later in more detail), and thus the different modes are reflected by the plates without mixing one with another.

Under the standard approach, the total zero-point energy in the cavity is calculated as a sum over the ground energies of all the quantum oscillators in the system:

$$\mathcal{E} = (\hbar/2) \sum [\omega_{\text{TM}}^{n_x, n_y, n_z} + \omega_{\text{TE}}^{n_x, n_y, n_z} + \omega_{\text{TEM}}^{n_x, n_y, n_z}]. \quad (4)$$

Besides the fact that this sum is terribly divergent, we realize that the contributions from the TE, TM, and TEM modes are all independent. These contributions may have, therefore, different behavior with respect to the length of the cavity a .

We start with the most interesting part: the contribution of the TEM modes. From Eq. (3), one can see that the zero-point energies of the quantum oscillators associated with these modes are independent of k_x and k_y . The number of oscillators associated with TEM modes is exactly N , where N is the number of wires in the cavity. This can be understood by noting that the wire medium may be regarded as a multiwire transmission line, and since each wire can be set to a unique electrostatic potential, there exist exactly N independent TEM modes in the cavity. Having this in mind, we may write the contribution of the TEM modes to the zero-point energy as follows: $\mathcal{E}_{\text{TEM}} = (\hbar c/2)(L^2/A_{\text{cell}}) \sum_{n_z=1}^{\infty} (\pi n_z/a)$, where $A_{\text{cell}} = b^2$ is the area of the transverse unit cell, and the coefficient $L^2/A_{\text{cell}} \equiv N$ gives the total number of independent TEM modes in the cavity. Performing a ζ regularization of the above sum, we find the interaction part of the zero-point energy: $\delta\mathcal{E}_{\text{TEM}} = N(\pi\hbar c/2a)\zeta(-1) = -N(\pi\hbar c/24a)$, where we used the fact that the Riemann ζ function verifies $\zeta(-1) = -1/12$. Thus, the force per unit area acting on the plates is

$$\frac{F_{\text{TEM}}}{L^2} = \frac{\pi}{24} \frac{\hbar c}{a^2 b^2}. \quad (5)$$

Here, we follow the same convention as in [1]: a positive force corresponds to attraction and a negative force corresponds to repulsion.

The obtained result reminds one of the Casimir force in inherently one-dimensional structures [9,13,14]. Specifically, in Ref. [13] the contribution of the TEM mode in a coaxial cylindrical cavity with a nonsimply connected cross section was calculated and the characteristic $1/a^2$ behavior was demonstrated, but the role of the TEM mode was found to be negligible when compared to the role of the other modes of the cavity. However, in the wire media that we consider in this paper the situation is completely different. In (5) there is an additional parameter which is not present in one-dimensional cases: it is the wire separation b . When this separation decreases the force increases, even if the metal volume fraction in the wire medium is kept invariant. Effectively, the TEM modes of a uniaxial wire medium act as many independent unidimensional “channels” that contribute equally to the total force (since the associated quantum harmonic oscillators have the same zero-point energy) boosting its intensity. The larger is the number of channels per unit of area; the stronger is the attraction between the plates. Thus, when a dense wire medium is placed in between two conducting plates it may effectively act as a “quantum super glue.” Interestingly, for PEC nanowires the F_{TEM} component of the force depends neither on the specific arrangement of the wires (which could be random) nor on the wire radius. A detailed analysis described in Sec. IV shows that for nanowires made of a realistic metal there is some dependence of the force on the radius, but this dependence is very weak provided the radius is larger than the metal skin depth in the infrared domain (a few tens of nanometers).

The TEM component of the Casimir force (5) was derived assuming that the nanowires are in electrical contact with the plates and considering the electromagnetic modes of the

resonator formed by the nanowires and the plates. While in most situations an electrical contact implies a mechanical contact, this does not necessarily imply that such a contact should prevent the relative movement of the plates and, therefore, the measurement of the Casimir force in the configuration of Fig. 1. One can imagine a configuration in which the nanowires penetrate one of the plates through holes while touching the walls of the holes and maintaining an electrical contact. In fact, a similar requirement is also present in the Casimir piston problem where the sliding plate must be in electrical contact with the lateral walls of a metallic waveguide [17,18]. In our geometry the situation is formally identical except that our sliding plate is perforated by the nanowires. Even touching the wires may not be necessary, because on a nanoscale the electrons can tunnel through narrow gaps providing in this way an electrical connection. Yet another possibility is that one of the metallic plates is a conducting liquid (e.g., liquid metal) where the wires attached to the other (solid) conducting plate are immersed. Moreover, from the physical point of view, even if the relative movement of the plates is limited, the Casimir energy is still there and can in principle be measured. For instance, the considered Casimir force between two metallic plates may manifest itself via a dramatic increase of the binding energy of the plates when the nanowires are present.

It is instructive to give here also an alternative derivation of the same force using the generalized Lifshitz formula [9,10]. With this approach it is possible to generalize (5) to the case where the conducting plates are replaced by homogeneous dielectrics or magnetics and the nanowires are prolonged into the materials. For this case, the contribution to the Casimir force by the m th dispersion branch of wire medium (seen as a photonic crystal) can be written as

$$\frac{F_m}{L^2} = \frac{2\hbar c}{\pi} \iint \frac{d^2 \mathbf{k}_\parallel}{(2\pi)^2} \frac{d}{da} \int_0^\infty \log(1 - r_1 r_2 e^{-2\gamma a}) d\xi, \quad (6)$$

where r_1 and r_2 are the reflection coefficients at the boundaries and $\gamma = -ik_z^{(m)}(\xi, k_x, k_y)$ and the double integration is done over the first quadrant of the Brillouin zone, $[0, \pi/b] \times [0, \pi/b]$. Within the framework of the continuous material model, $\gamma = \sqrt{\xi^2 + k_p^2 + k_x^2 + k_y^2}$ for the first TM branch, and $\gamma = \sqrt{\xi^2 + k_x^2 + k_y^2}$ for the first TE branch [Eqs. (1) and (2)].

For the TEM mode, $\gamma = \xi$ and the reflection coefficients are independent of k_x and k_y and determined by the effective impedances of the adjacent materials: $r_{1,2} = (\eta_{1,2} - \eta_0)/(\eta_{1,2} + \eta_0)$. Hence, if the material dispersion is negligible in the region $\xi \lesssim 1/a$ that contributes the most to the integral (6), the force due to the TEM waves is

$$\frac{F_{\text{TEM}}}{L^2} = \frac{\hbar c}{4\pi a^2 b^2} \int_0^\infty \frac{t dt}{e^{t/(r_1 r_2)} - 1} = \frac{\hbar c \text{Li}_2(r_1 r_2)}{4\pi a^2 b^2}, \quad (7)$$

where $\text{Li}_2(z) = \sum_{n=1}^\infty z^n/n^2$ and the reflection coefficients are assumed constant. Equation (7) reduces to (5) when $r_1 r_2 = 1$ (e.g., a pair of highly conducting or highly permeable plates). Since the polylogarithm function is such that $\text{Li}_2(x) < 0$ for $x < 0$, it follows that when $r_1 r_2 < 0$ the Casimir force is repulsive. In particular, a long-range repulsive force may be obtained when a conducting plate is combined with a permeable plate, or alternatively, as discussed ahead, when the nanowires are embedded in three nonmagnetic materials

with $\varepsilon_1(i\xi) < \varepsilon_2(i\xi) < \varepsilon_3(i\xi)$, which corresponds to a generalization of Dzyaloshinskii's configuration [3].

The contribution of the TE and TM modes can also be obtained with the help of Eq. (6). The only difference as compared to the TEM case is the expression of γ in the exponential term. Given that Eq. (6) is often derived with a scattering formalism and that in our system the wires are in contact with the plates, this may be somehow surprising for someone accustomed to the fact that scattering theories apply only to spatially separated bodies. However, it can be shown that the integral (6) is completely equivalent to a regularized summation of the zero-point energies of the respective electromagnetic modes in a cavity (this can be easily done with the help of the argument principle [19,20]). The same can be also seen from the fact that we have done such a direct summation for the TEM case and obtained a result that is in perfect agreement with (7). Clearly, the summation of the zero-point energies in a cavity [and therefore Eq. (6) that can be derived from such a summation with the argument principle] does not suffer from the limitations of the scattering theories, because it is based on a completely independent approach.

In order to obtain the TM component of the force, we note that since $\exp(-2\gamma a)$ is quickly decaying for TM waves, the double integration over k_x and k_y in Eq. (6) can be extended to the first quadrant of the (k_x, k_y) plane. Introducing polar coordinates, it is easily found that (for $r_1 r_2 = 1$)

$$\frac{F_{\text{TM}}}{L^2} = \frac{\pi^2 \hbar c}{480 a^4} \left[1 - \frac{60}{\pi^4} \int_0^{(k_p a)^2} \int_0^\infty \frac{q dv dw}{e^q - 1} \right], \quad (8)$$

where $q = 2\sqrt{v^2 + w}$. When $k_p a \rightarrow 0$ (i.e., when $r_0/b \rightarrow 0$ so that the nanowires are very diluted), Eq. (8) reduces to one-half of the Casimir force between two conducting plates in vacuum. The expression in square brackets is positive and less than unity, and monotonically decreases when $k_p a$ increases. Therefore, the TM contribution is a short-range force that decays with distance faster than $1/a^4$. This is illustrated in Fig. 1, where the ratio $F_{\text{TM}}/F_{\text{TEM}}$ is plotted as a function of the relative separation a/b .

The final contribution to the Casimir force is due to the TE modes. Within the framework of the continuous material model [Eq. (1)], the dispersion of these ordinary waves is the same as in vacuum. Indeed, the TE polarized waves do not interact with the thin wires, because the wires are orthogonal to the electric field. Thus, the contribution of the TE modes, F_{TE} , is exactly one-half of the Casimir force between a pair of plates in vacuum. This force is also short range, as is seen from Fig. 1. In particular, remembering that F_{TE} is approximately one-half of the force in the absence of the nanowires, Fig. 1 demonstrates that the intensity of the Casimir force (mainly determined by F_{TEM}) is indeed boosted at long distances when the nanowires are present. The enhancement of the force caused by the presence of the nanowires may seem surprising if one remembers that in the configuration studied by Lifshitz the addition of an isotropic material in between the plates depresses the force. However, a wire medium is a strongly anisotropic material which explains the different behaviors.

III. COMPARISON WITH FULL-WAVE SIMULATIONS

It is interesting to compare the Casimir force calculated using the effective medium model with a full-wave simulation that takes into account all the details of the microstructure of the system. In this section, we make such a comparison assuming as in Sec. II that the metals are perfect conductors and that the wires are in electrical contact with the plates.

A crucial point is that under this assumption the formula derived for the TEM component of the force [Eq. (5)] is actually *exact*. This should be evident from the fact that it was calculated based on the regularized summation of the zero-point energies of the respective electromagnetic modes in a cavity, and that Eq. (3) is the exact dispersion of the TEM modes in a wire crystal with perfectly conducting wires. Thus, within the framework of the full wave calculation, we only need to worry with the TE and TM components of the force.

As detailed in Appendix A, the contributions of the TE and TM modes can be calculated using the generalized Lifshitz formula (6), with the exact dispersion $\gamma = \sqrt{\xi^2 + \beta_i^2(k_x, k_y)}$ of the TE and TM modes.

Specifically, in order to calculate the full wave TE and TM components of the force the first Brillouin zone was sampled with 39×39 pairs of (k_x, k_y) values, and for each such pair the corresponding $\beta_i(k_x, k_y)$ was found for the 20 lowest TE and TM wire medium bands using the method reported in [21]. For each branch, the integral over (k_x, k_y) in (6) was approximated by a summation [see Eq. (A3) of the Appendix]. The remaining integration over the imaginary frequency was done numerically. Then, the total force was found as the sum of the modal forces. The obtained results are represented in Fig. 1 with discrete symbols, confirming that the continuous medium approximation works extremely well, especially for the TM modes. The small disagreement in the contribution of the TE modes is related to the fact that we have neglected the transverse polarizability of the wires.

IV. EFFECT OF FINITE CONDUCTIVITY OF NANOWIRES AND PLATES

Equation (7) shows that the perfect electrical conductor approximation for the plates is not critical for the long-range Casimir force. Indeed, it follows from Eq. (7) that if the metal plates are replaced by dielectrics (with the wires penetrating into them), the ultralong-range behavior of the force remains the same, even though the magnitude of the force may be weaker. For instance, from Eq. (7) the TEM component of the force between two silica plates embedded in PEC nanowires is 2% of the TEM component of the force between two PEC plates [note that $(6/\pi^2)\text{Li}_2(r_1 r_2) = (6/\pi^2)\text{Li}_2((\sqrt{\epsilon_r} - 1)/(\sqrt{\epsilon_r} + 1)^2) \approx 0.02$; following [5] the permittivity of silica is $\epsilon_r(i\xi) \approx 2.08$ and varies insignificantly with $i\xi$]. Although the force is significantly weaker than in the PEC case, it still has the characteristic $1/a^2$ behavior.

A similar estimation can be done for the plates made of a realistic metal. As the Casimir force grows with the reflectivity of the plates [i.e., with the value of $\epsilon_r(i\xi)$], we can obtain a lower-bound estimate for the force if we consider the minimal value of $\epsilon_r(i\xi)$ in the frequency range of interest: $\xi \lesssim 1/a$. The minimal value of the permittivity in this range is achieved at

$\xi = 1/a$ [it is a consequence of the Kramers-Kronig relations that $\epsilon_r(i\xi)$ is a monotonically decreasing function of ξ]. Thus, for $a = 10 \mu\text{m}$ we have $\xi_{\text{max}} = 10^5 \text{ m}^{-1}$ which corresponds to $|\omega_{\text{max}}| \approx 3 \times 10^{13} \text{ rad/s}$. The permittivity of silver at this (imaginary) frequency can be calculated from a Drude model with the parameters taken from the experimental data of Ref. [22] and is about $\epsilon_r(i\xi_{\text{max}}) \approx 10^5$, that is, the reflection coefficient of the TEM modes at this frequency is $r_{1,2} = -(\sqrt{\epsilon_r} - 1)/(\sqrt{\epsilon_r} + 1) \approx -0.9937$ and the respective reduction in the Casimir force due to the finite conductivity of the plates is $1 - (6/\pi^2)\text{Li}_2(r_1 r_2) \approx 0.04$ (i.e., the reduction is only about 4%). It is interesting to note, however, that at shorter distances the reduction is higher. For instance, at $a = 1 \mu\text{m}$ one should consider $|\omega_{\text{max}}| \approx 3 \times 10^{14} \text{ rad/s}$, and the same very conservative calculations predict a 20% reduction of the force when compared to PEC plates. The explanation of this phenomenon is that at shorter distances the modes with higher frequencies contribute more to the force, and these modes are more affected by the nonideality of the plates. Thus, at large separations it is the finite conductivity of the nanowires (and not that of the plates) that may limit the intensity of the Casimir force. Next, we study the effect of loss and dispersion in the nanowires, supposing that the plates are either dielectrics or PEC.

In order to estimate the effect of loss and dispersion in nanowires made of real metals, we calculated the Casimir force by direct numerical integration of (6) using a suitable effective medium model for the silver nanowires [16,23]. Interestingly, the results of our theoretical model indicate that the effect of loss and dispersion is quite mild and that the results obtained using the PEC assumption describe well the physics of the system. Indeed, in Fig. 2 we compare the results obtained based on the PEC approximation and the results obtained for realistic silver wires (silver is described by the Drude model [22], as above), considering configurations similar to those of the

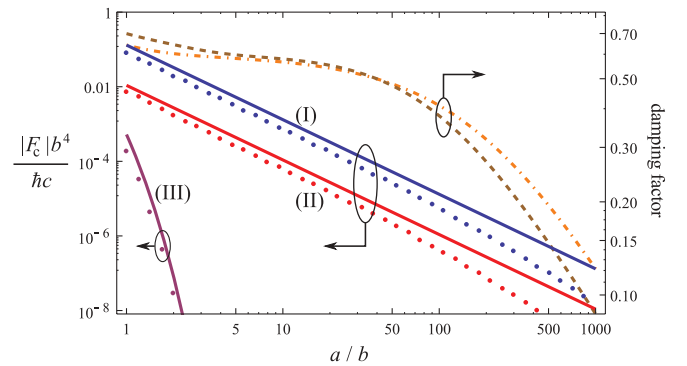


FIG. 2. (Color online) (Left scale) The Casimir forces due to the quasi-TEM modes [the blue line and dots (I)] and the TM modes [the violet line and dots (III)] as functions of the distance between the PEC metal plates in the configuration shown in the inset of Fig. 1. Solid lines, lossless case; dots, lossy and dispersive silver wires modeled through the experimental data of Ref. [22]. The red line and the dots (II) are the same as (I) but for a metal-bromobenzene-air configuration (inset A of Fig. 4). (Right scale) Attenuation in the Casimir force (relative to the PEC case) for silver nanowires. Brown dashed line, parallel plate geometry with metallic reflecting walls (as in Fig. 1); orange dot-dashed line, metal-bromobenzene-air configuration (inset A of Fig. 4). In all these plots, $r_0 = 20 \text{ nm}$, $b = 100 \text{ nm}$.

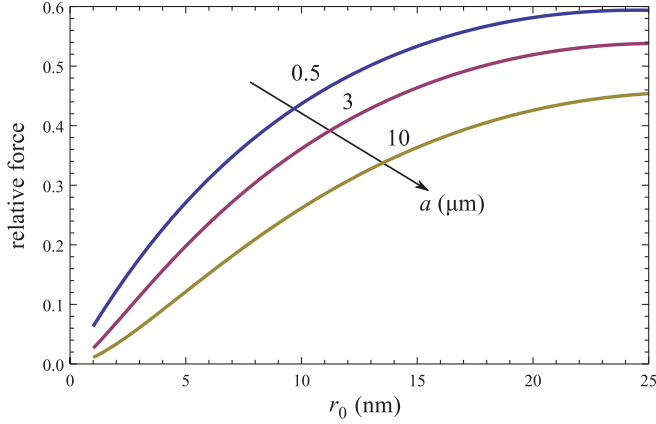


FIG. 3. (Color online) The Casimir force between two conducting plates embedded in a silver nanowire background as a function of the radius of the nanowires (normalized to the same force with PEC nanowires). The value of the plate separation a is indicated in the legend and $b = 100$ nm.

example of Fig. 1. The wires have radius $r_0 = 20$ nm and are spaced by $b = 100$ nm. As can be seen, the difference between the two cases is quite modest in logarithmic units. In particular, it can be seen that the variation of the force with distance follows practically the same trend both in the ideal case as well as in the case that takes into account the loss and the dispersion. The forces between conducting or dielectric plates (the latter configuration will be further discussed in Sec. V) were found to be roughly one-half of the forces predicted by (5) and (7) in the range $1 \leq a/b \leq 100$ with the characteristic $1/a^2$ behavior confirmed for distances as large as $10 \mu\text{m}$. This demonstrates the robustness of the mechanism proposed in this work to enhance the intensity of the Casimir force. At larger distances the force decays faster, but becomes practically immeasurable due to its very low absolute value.

We have also studied the dependence of the Casimir force on the radius of the nanowires. While for PEC nanowires the TEM contribution to the force is completely independent of the radius, in the case of nanowires made of a realistic metal there is some dependence of the force on the radius. However, this dependence is quite weak provided the radius is larger than the metal skin depth (which is about 20 nm for silver in the infrared domain). For the case when the wire radius approaches the skin depth, the dependence of the force on the radius is shown in Fig. 3. As is seen, with the parameters given in the figure the curves do not reach unity. This is expected as for such small lattice periods and such thin plasmonic wires, the average z component of the phase velocity of the quasi-TEM waves with different \mathbf{k}_{\parallel} is less than the speed of light, $v_{\text{ph}} < c$, and from (5) it can be inferred that the force is roughly proportional to this average phase velocity.

We would like to point out that this robustness to the effect of loss and dispersion is consistent with several recent theoretical and experimental studies about the imaging properties of nanowires, which demonstrated that even in the infrared and optical domains the nanowire array may be able to transport an electromagnetic signal with relatively low absorption (see, e.g., [11,12,24]). In this work, we take advantage of such property to

channel the quantum fluctuations of the electromagnetic field and in this manner to boost the range of the Casimir force.

V. POSSIBLE EXPERIMENTS

We would like to speculate on a possible experimental verification of this theory. One can imagine the setup outlined in the inset A of Fig. 4, which represents a dielectric liquid (e.g., bromobenzene [5] at room temperatures or liquid He [25] at very low temperatures) embedded in the nanowires and backed by a conducting plane (the nanowires are extended into the air region as shown). Assuming that the permittivities of the conducting plate, the liquid and the air region, verify $\varepsilon_1(i\xi) > \varepsilon_2(i\xi) > \varepsilon_3(i\xi)$, it follows from our theory that the force acting on the liquid is repulsive, forcing it to climb the nanowires. Since the force is long range, this effect may be observed even for relatively large values of a , (see curve II of Fig. 2), even though it may be challenging to distinguish it from the effect of the capillary forces.

The capillary force due to a single wire in our system is proportional to the perimeter of the wire $2\pi r_0$. Therefore, the effect of the capillary forces per square meter is $(F_{\text{cap}}/A_{\text{cell}}) = (2\pi r_0)\sigma \cos \theta / b^2$, where σ is the surface tension of the liquid and θ is the wetting angle for the specific combination of the liquid and the material of the wires. The capillary force can be reduced with surfactants or when operating close to the critical point of a liquid. This force per unit of area in our configuration has the same dependence on the unit cell size as the Casimir force, but does not depend on the plate separation a . It may be feasible that such a distance-independent force may be compensated by gravitational or inertial forces or perhaps by applying certain constant pressure to the liquid. Another important point is that the capillary force decreases with the radius of the wires, while the Casimir force practically does not depend on the radius of the wires provided that the

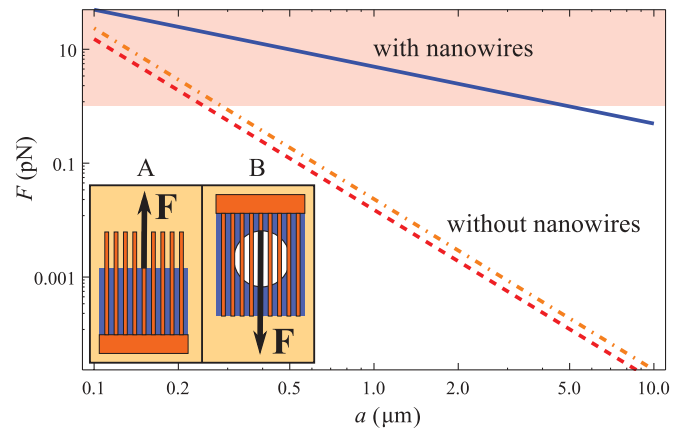


FIG. 4. (Color online) Casimir force between a metal plate and an air bubble (radius $20 \mu\text{m}$) immersed in bromobenzene in a wire medium background (inset B), as a function of their separation. Blue solid line, absolute value of repulsive force in the presence of nanowires; red dashed line, the same without the wires; orange dot-dashed line, the attractive force between a gold sphere (radius $20 \mu\text{m}$) and a gold plate immersed in bromobenzene as in [5]. The shading shows the range of forces measured in [5]. The parameters are the same as in Fig. 2.

radius is larger than the skin depth. Thus, the postprocessing of experimental data obtained for samples with different r_0/b ratio may also help in extraction of the distance-dependent part of the total force.

There may be, however, a simple way to effectively cancel out the contribution from the surface tension forces. Specifically, one may consider an air bubble of radius $R \gg b$ embedded in the liquid and nanowires and measure the total repulsive force acting on it (inset *B* of Fig. 4). It is obvious that the capillary forces acting on the opposite sides of a bubble cancel out each other. However, the stability of such a bubble when embedded into an array of nanowires may be of concern. In Appendix B we present theoretical and numerical arguments that suggest that a large enough bubble is stable when immersed in a periodic array of nanowires.

When R is much greater than the separation between the bubble and the metal plate a , the Casimir force acting on the bubble can be found from (7) using the proximity theorem [4] as $F_{ps}(a) = (2\pi R)(\hbar c/4\pi ab^2) \text{Li}_2(r_1 r_2) \propto 1/a$. Thus, in the presence of the nanowires, this force is very long range as seen from the plots in Fig. 4 for a bubble with radius $20 \mu\text{m}$: if an apparatus with the same sensitivity as in [5] was used, it would be possible to consider distances as large as $10 \mu\text{m}$! In the absence of the nanowires, the force is much weaker at long distances and is proportional to $1/a^3$.

VI. CONCLUSIONS

To conclude, we have considered Casimir's attractive and repulsive forces acting on bodies immersed in uniaxial wire media. We have found that in these structures the Casimir's forces are ultralong range, and decay in parallel plate configurations as $1/a^2$, and in sphere-parallel plate configurations as $1/a$, while the same forces in an isotropic background behave as $1/a^4$ and $1/a^3$, respectively. This dependence of the force on distance may remind one in part of some 1D systems, however, unlike in 1D systems the configuration proposed here is fully three-dimensional (3D), and in particular enables the interaction between complex 3D bodies embedded in the nanowire background. It was shown that when compared to vacuum or even local uniaxial dielectrics, a nanowire array supports waves whose dispersion is independent of \mathbf{k}_{\parallel} , and thus the corresponding quantum oscillators contribute all equally to the Casimir force, greatly enhancing its intensity at large separations. For one of the configurations considered in this work, with realistic material parameters and the effect of loss taken into account, our calculations show that the Casimir forces mediated by wire media may be measurable up to $10\text{-}\mu\text{m}$ distances.

APPENDIX A

In this appendix we describe how the Casimir force can be obtained using a full wave simulation for the geometry of the inset of Fig. 1. It is assumed that all the metals are PEC and that the nanowires are in contact with the metallic plates. Thus, we deal with a periodic structure made of PEC objects that are uniform along the z axis (2D photonic crystal). It is well known that the electromagnetic modes in such a structure can be classified into three types, as already discussed in the

main text: TEM, TM, and TE. Because of the translational symmetry of the structure with respect to the z axis, it is well known that the dispersion characteristic of the TE and TM modes is *exactly* of the form,

$$\frac{\omega^2}{c^2} = \beta_{n,\alpha}^2(k_x, k_y) + k_z^2, \quad \alpha = \text{TE, TM}, \quad (\text{A1})$$

where $\beta_{n,\alpha}(k_x, k_y)$ are the resonant wave numbers of the electromagnetic modes ($n = 1, 2, 3, \dots$) for the case $k_z = 0$ (i.e., the cutoff wave numbers), and (k_x, k_y, k_z) is the wave vector associated with the Bloch modes. The cutoff wave numbers $\beta_{n,\alpha}(k_x, k_y)$ are not known, but can be numerically computed.

The crucial point is that the modes with different (k_x, k_y) do not mix one with another upon reflection at the interfaces (PEC walls), and thus their contribution to the Casimir force can be calculated independently, and is additive. Moreover, the reflection coefficient at the PEC walls is exactly -1 for every mode (this happens due to the invariance of the structure along z and because the wires are connected to the PEC plates).

Hence, the contribution to the Casimir energy due to the cavity modes associated with a given branch (n) of TE or TM modes for a fixed (k_x, k_y) can be individually calculated using the Lifshitz formula through the following exact formula:

$$\delta\mathcal{E}_{n,\alpha} = \frac{\hbar c}{2\pi} \int_0^\infty \log(1 - e^{-2\gamma_{n,\alpha}a}) d\xi, \quad (\text{A2})$$

where $\gamma_{n,\alpha} = -ik_z$ is the solution of the dispersion Eq. (A1), for a fixed (k_x, k_y) and fixed $\omega/c = i\xi$. The key feature is that for the considered structure the dependence of $\gamma_{n,\alpha}$ on ξ can be easily determined as $\gamma_{n,\alpha} = -ik_z = \sqrt{\beta_{n,\alpha}^2 - \omega^2/c^2} = \sqrt{\beta_{n,\alpha}^2 + \xi^2}$, and thus $\delta\mathcal{E}_{n,\alpha}$ may be easily evaluated numerically. The use of the Lifshitz formula can be justified by noting that it yields exactly the regularized summation of the zero-point energies associated with the considered branch of TE or TM modes and (k_x, k_y) , as can be verified using, for example, the argument principle [19,20].

Since the contributions of the modes are additive, we have

$$\delta\mathcal{E} = \sum_{k_x, k_y} \sum_{n,\alpha} \delta\mathcal{E}_{n,\alpha}. \quad (\text{A3})$$

In the continuous case, the sum over (k_x, k_y) becomes an integral, and can be written as

$$\begin{aligned} \frac{\delta\mathcal{E}}{L^2} &= \sum_{n,\alpha} \frac{\hbar c}{2\pi^3} \int_0^{\pi/b} \int_0^{\pi/b} dk_x dk_y \\ &\times \int_0^\infty \log(1 - e^{-2\gamma_{n,\alpha}a}) d\xi. \end{aligned} \quad (\text{A4})$$

We emphasize that this expression for the Casimir energy is an exact result that has been derived taking into account all the details of the microstructure of the system.

APPENDIX B

The problem of stability of a bubble in a nanowire background can be attacked as follows. Under isothermal, isobaric conditions, the Gibbs free energy of a large (compared

to the separation of the nanowires) air bubble immersed in the wires can be written as

$$G = \sigma S_a + \sigma \cos \theta S_w + (p_a - p_0) V_a, \quad (\text{B1})$$

where σ is the surface tension of the fluid, θ is the wetting angle for the specific combination of the fluid and the material of the wires, S_a is the surface of the air-fluid interface, S_w is the area of the air-metal interface inside the bubble (the surface of the wires), p_a is the air pressure inside the bubble, p_0 is the fixed outside pressure, and V_a is the total volume of air in the bubble.

The last term in the expression for G can be neglected for bubbles with diameters ranging from one up to hundreds of microns (which is the case of interest) that are placed under normal pressure. This is equivalent to assuming that both the internal pressure (which is about p_0) and the volume of the bubble do not change when its shape evolves. Under these assumptions, we can rewrite the Gibbs energy as

$$\begin{aligned} G &= \sigma_{\text{eff}} S_{\text{av}} + \sigma \cos \theta N (2\pi r_0) (V_{\text{av}} / A_p) \\ &= \sigma_{\text{eff}} S_{\text{av}} + (F_{\text{cap}} / b^2) V_{\text{av}}, \end{aligned} \quad (\text{B2})$$

where S_{av} is the area of the average surface of the bubble and $\sigma_{\text{eff}} = \sigma (S_a / S_{\text{av}})$ is the effective surface tension defined on this surface, respectively, V_{av} is the volume enclosed by this surface, N is the number of wires inside the bubble, and A_p is the area of the projection of the bubble onto a plane orthogonal to the wires, such that the quantity (V_{av} / A_p) gives the average height of the wires inside the bubble. Taking into account that $N / A_p = 1 / b^2$ and $2\pi r_0$ is the circumference of a single wire, we arrive at the final expression in which the constant quantity $(F_{\text{cap}} / b^2) = \sigma \cos \theta (2\pi r_0) / b^2$ is the capillary pressure per unit cell of wire medium. Under our assumptions V_{av} is also a constant, therefore, the minimum of the free energy is achieved

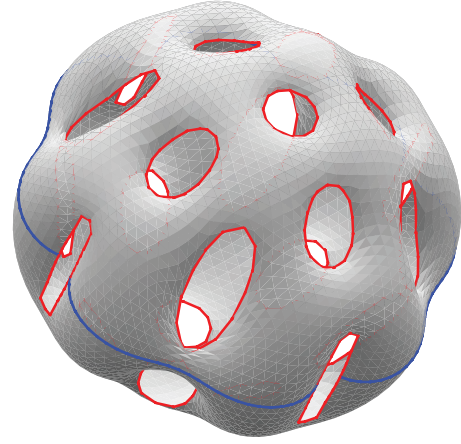


FIG. 5. (Color online) The simulated surface of a bubble in a periodic wire medium background after 500 iterations of the algorithm of Ref. [26]. The bubble is initially an ideal sphere of radius $R/b = 11/6$, perforated with wires of radius $r_0/b = 1/4$. The wetting angle at the wire surface is $\theta = 30^\circ$.

at the minimum of the average surface S_{av} [i.e., when the bubble is (on average) a sphere].

To check this simple theoretical argument we simulated a bubble immersed in an array of wires with the software SURFACE EVOLVER [26]. The results of simulations show that a large air bubble in an infinite periodic array of wires is stable, while the same bubble pierced with just a few wires is not: in the last case the bubble is pressed in the direction of wires and tries to escape the wires. In other words, in a periodic array of wires the bubble is stable simply because it does not have a place to escape. Figure 5 shows an example of the simulated shape.

-
- [1] H. B. G. Casimir, Proc. K. Ned. Akad. Wet. **51**, 791 (1948).
 - [2] E. M. Lifshitz, Sov. Phys. JETP **2**, 73 (1956).
 - [3] I. E. Dzyaloshinski, E. M. Lifshitz, and L. P. Pitaevski, *Adv. Phys.* **10**, 165 (1965).
 - [4] S. K. Lamoreaux, *Phys. Rev. Lett.* **78**, 5 (1997).
 - [5] J. N. Munday, F. Capasso, and V. A. Parsegian, *Nature (London)* **457**, 170 (2009).
 - [6] U. Leonhardt and T. G. Philbin, *New J. Phys.* **9**, 254 (2007).
 - [7] R. Zhao, J. Zhou, T. Koschny, E. N. Economou, and C. M. Soukoulis, *Phys. Rev. Lett.* **103**, 103602 (2009).
 - [8] V. Yannopapas and N. V. Vitanov, *Phys. Rev. Lett.* **103**, 120401 (2009).
 - [9] K. A. Milton, *The Casimir Effect: Physical Manifestations of Zero-Point Energy* (World Scientific Publishing, Singapore, 2001).
 - [10] F. S. S. Rosa, D. A. R. Dalvit, and P. W. Milonni, *Phys. Rev. Lett.* **100**, 183602 (2008).
 - [11] P. A. Belov, Y. Zhao, S. Tse, P. Ikonen, M. G. Silveirinha, C. R. Simovski, S. Tretyakov, Y. Hao, and C. Parini, *Phys. Rev. B* **77**, 193108 (2008).
 - [12] M. G. Silveirinha, P. A. Belov, and C. R. Simovski, *Opt. Lett.* **33**, 1726 (2008).
 - [13] E. Álvarez and F. D. Mazzitelli, *Phys. Rev. D* **79**, 045019 (2009).
 - [14] D. Zhabinskaya and E. J. Mele, *Phys. Rev. B* **80**, 155405 (2009).
 - [15] P. A. Belov, R. Marques, S. I. Maslovski, I. S. Nefedov, M. Silveirinha, C. R. Simovski, and S. A. Tretyakov, *Phys. Rev. B* **67**, 113103 (2003).
 - [16] S. I. Maslovski and M. G. Silveirinha, *Phys. Rev. B* **80**, 245101 (2009).
 - [17] R. M. Cavalcanti, *Phys. Rev. D* **69**, 065015 (2004).
 - [18] M. P. Hertzberg, R. L. Jaffe, M. Kardar, and A. Scardicchio, *Phys. Rev. Lett.* **95**, 250402 (2005).
 - [19] A. Lambrecht and V. N. Marachevsky, *Phys. Rev. Lett.* **101**, 160403 (2008).
 - [20] K. Schram, *Phys. Lett. A* **43**, 282 (1973).
 - [21] M. G. Silveirinha and C. A. Fernandes, *IEEE Trans. Microwave Theory Tech.* **51**, 1460 (2003).
 - [22] M. A. Ordal, R. J. Bell, J. R. W. Alexander, L. L. Long, and M. R. Query, *Appl. Opt.* **24**, 4493 (1985).
 - [23] M. G. Silveirinha, *Phys. Rev. E* **73**, 046612 (2006).
 - [24] J. Yao, Z. Liu, Y. Liu, Y. Wang, C. Sun, G. Bartal, A. Stacy, and X. Zhang, *Science* **321**, 930 (2008).
 - [25] E. S. Sabisky and C. H. Anderson, *Phys. Rev. A* **7**, 790 (1973).
 - [26] K. A. Brakke, *The Surface Evolver* [<http://www.susqu.edu/brakke/evolver/evolver.html>].